The Geographic Base

Journal Homepage: https://www.ngssnepal.org/journal

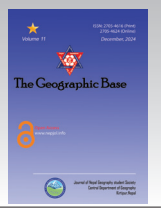

Geospatial Modeling of the Drivers of Land Surface Temperature in Salyan District: Application of GWR

Bijaya Kafle
Central Department of Geography, Tribhuvan University.
Email: bijayakafle04@gmail.com

Article info

Keywords:
land surface temperature, GWR, topography, GEE

Received: 7th July. 2024

Accepted: 15th Oct. 2024

DOI: https://doi.org/10.3126/tgb.v11i01.88564

Abstract

Land Surface Temperature (LST) is an important component of surface energy balance, microclimate modulation, hydrological cycles, vegetation productivity, and human wellbeing. Thus, a spatial knowledge of its variation and drivers is essential in mountainous country like Nepal, where topographic complexity and heterogeneous land use create strong thermal contrasts. This paper explored the geospatial determinants of LST in Salyan District, Nepal, using Geographically Weighted Regression (GWR). The dependent variable of the study, LST, was exported from the MODIS through Google Earth Engine platform, while elevation, slope, solar radiation, and proximity to streams were derived from SRTM DEM. Building point density was extracted from OpenStreetMap. The results showed that the GWR substantially enhanced the explanation of spatial heterogeneity, with $R^2 = 0.939$ and Adjusted $R^2 = 0.915$, outperforming global regression models. Moran's I Spatial residual analysis (Index=0.092, Z=2.98, p=0.0028) also indicated a statistically significant clustering but within an acceptable level for spatial modeling. The present study brings forth location-specific

influences of topography, anthropogenic factors, and radiation dynamics on LST, and it shows the applicability of GWR for climate-sensitive planning and resource management in Nepal's mid-hill districts.

Introduction

Land surface temperature is an important parameter that connects land-atmosphere energy exchanges, local climate, and environmental processes as evapotranspiration, soil moisture dynamics, and urban heat island development. Complex topography, diverse land cover, and rapid socioeconomic change in mountainous places, such as Nepal, generate substantial spatial disparities in LST that traditional global regression models, which presume spatial stationarity, cannot capture. Salyan District in western Nepal's hilly region has difficult terrain, scattered rural settlements, and rising minor urban centers, making it an ideal environment to study how biophysical and built-up elements influence LST patterns (Li et al., 2022; Roba et al., 2025).

GWR has emerged as a powerful approach to model spatially varying relationships between LST and its drivers are calibrated using local regression coefficients for each place rather than a single global equation (Wang et al., 2022). Previous research has used GWR to investigate urban heat islands (Roba et al., 2025), LST & land cover interactions (Zhi et al., 2019) and downscaling of thermal satellite data, demonstrating that predictors such as elevation, vegetation, impervious surfaces, and radiation frequently change significantly over space. However, GWR applications in Nepal's mid-hill districts are limited, particularly those that integrate topographical factors with built-up indicators acquired from open geospatial data (Lessani et al., 2024;).

This study aims to fill this gap by developing a geospatial model of LST drivers in Salyan district using GWR with MODIS-derived LST as the dependent variable and elevation, slope, solar radiation, building density and distance to streams as explanatory variables. Specifically, the objectives are to (i) map the spatial distribution of LST using MODIS data, (ii) derive terrain and hydrological variables from Shuttle Radar Topography Mission (SRTM) digital elevation data, (iii) incorporate building information from OpenStreetMap (OSM) as a proxy for built-up intensity, and (iv) quantify and interpret the spatial heterogeneity in the relationships between LST and its drivers. The study further evaluates model adequacy using global measures of fit and spatial autocorrelation of residuals.

Methods and Materials

Study area

The Salyan Districtis of Karnali Province of Nepal is taken as the study area due to its rugged landscape with elevations ranging approximately from low river valleys to high ridges, which produce substantial variations in slope, aspect

and solar exposure (Figure 1). Settlement patterns range from dense market centers along transportation corridors to dispersed rural housing, while land cover includes agricultural terraces, forest, shrub land and built-up patches, all of which influence the local surface energy balance and, consequently, LST. The district's monsoon-dominated climate with pronounced dry and wet seasons further modifies LST through changes in soil moisture and vegetation phenology.

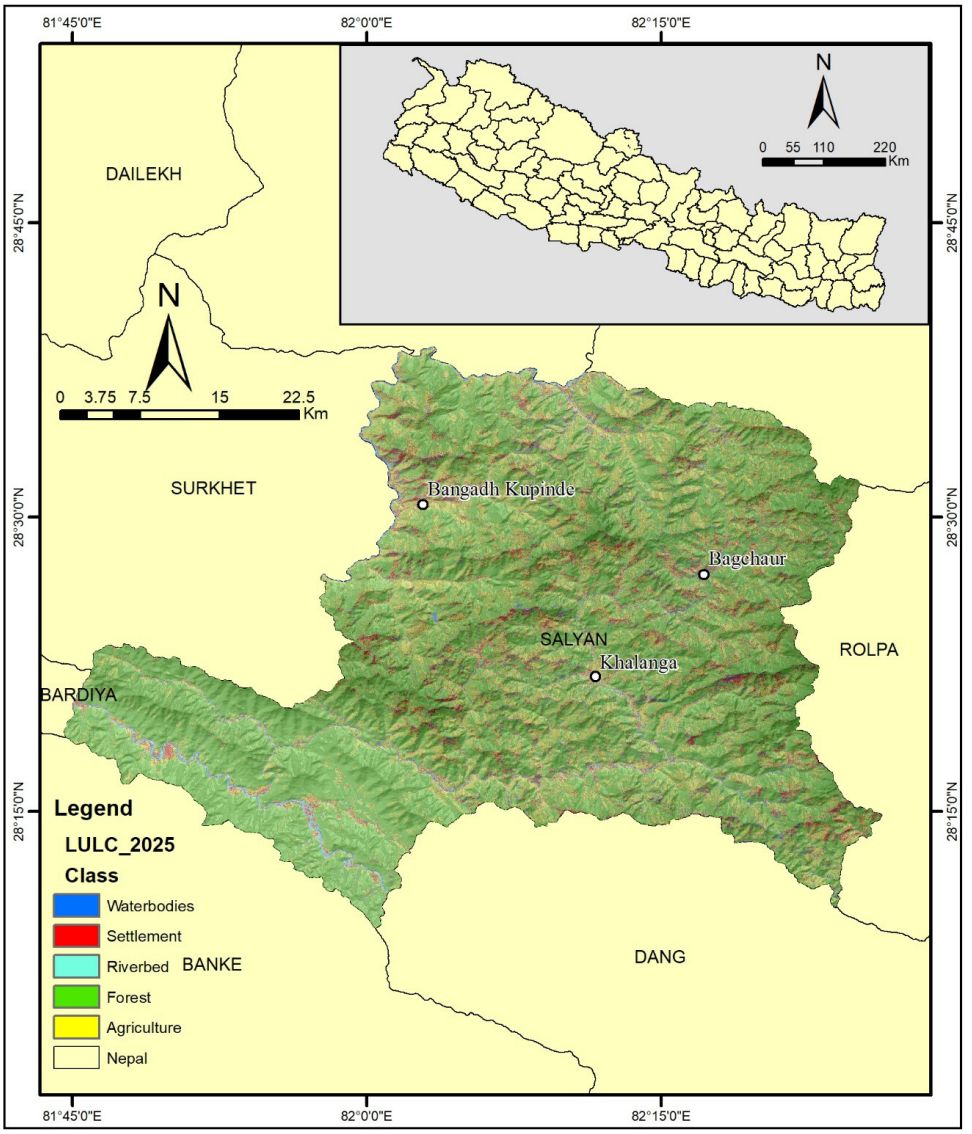

Figure 1. Salyan District

Data processing

Data adjustment and correction

All datasets were projected to a common coordinate system appropriate for spatial analysis in Nepal and resampled to a uniform grid resolution of 2 km compatible with the MODIS LST data. LST images were temporally composited, and pixels affected by clouds or low quality according to MODIS quality flags were masked to reduce retrieval errors. Terrain derivatives-slope and solar radiation index-were computed from the DEM using standard GIS algorithms (Seyoum 2024). Building points from OSM were filtered to keep those features categorized as residential, commercial, or mixed-use structures, before being spatially joined to the analysis grid to determine building counts or densities per cell.

Development of observation units

For the spatial statistical analysis of the observation units, the variables should be at the same location and compatible size of observation units (Kopczewska, 2025). Thus, one and two square kilometers grid maps were developed using fishnet function and intercepted both of them to the district boundary. Then, zonal statistics were done with all six variables (solar radiation, elevation, slope, building density, distance to streams and LST) in those two different grid maps in ArcGIS. The variables were normalized for numeric stability and comparability of coefficients. After running GWR models in both of those (1 km2 and 2 km2 zonal) maps separately, two kilometers square grid was found to be more suitable and reliable in term of coefficient of determinants and model validation. Thus, two-kilometer square grid was selected for the analysis.

Exploratory data analysis included inspection of distributions, correlation matrices, and diagnostics of multicollinearity necessary to ensure that the predictors were suitable for inclusion in regression modeling.

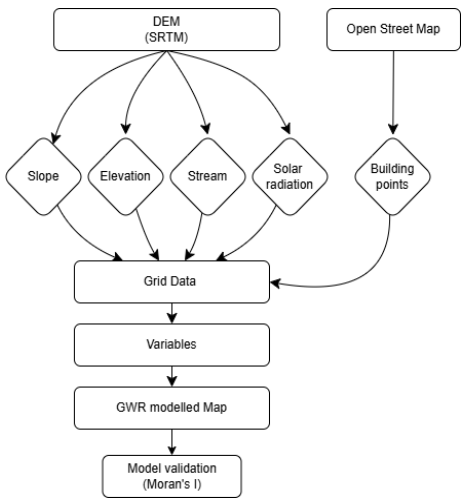

Figure 2. Methodological framework

Data source and variables

Dependent variable

The Land Surface Temperature (LST) was taken as the dependent variable. That was obtained from 8-day MODIS (Moderate Resolution Imaging Spectroradiometer) daytime LST data (MOD11A2) products based on a split-window algorithm (Rao et al. 2021; Hou et al. 2021; Yao et al. 2021). The LST data was from 2024 to 2025 at 1 km spatial resolution, provided by the National Aeronautics and Space Administration (NASA) and was later resampled at 2 km spatial resolution.

Independent Variable

Based on the available literature and data, this article selected five variables under four dimensions as the independent variables to analyze the spatial agglomeration effect of LST in Salyan District (see Table I).

Table 1. GWR table with each independent variables

S.N.	Variable type	Variables	Source
1.	Dependent variable	Land Surface Temperature	MODIS
2.	Independent variable	Slope	SRTM DEM
3.	Independent variable	Elevation	SRTM DEM
4.	Independent variable	Solar Radiation	SRTM DEM
5.	Independent variable	Stream network	SRTM DEM
6.	Independent variable	Building points	Open Street Map

Solar radiation: The heat absorption capacity of the surface is altered by the change in land cover. Buildings usually reduce the albedo and emissivity of surfaces, resulting in large surface heat storage in urban areas. Whereas vegetation with high albedos and high Bowen ratio may transmit little heat to the environment when exposed to solar radiation (S. Liang et. al 2021).

Topographical features: The terrain affects the storage of surface heat, in turn changing the intensity of LST (A.Guo et al. 2020)**.** The study used the SRTM Global Digital Elevation Model, which has a high spatial resolution of 30 m and is derived from NASA's USGS Earth Explorer. After executing the preprocess of projection transformation and surface analysis in ArcGIS 10.5, three topographical indicators were selected as independent variables: elevation, slope, and stream network.

Building points: These were obtained from OpenStreetMap, an open, volunteered geographic information database that has proven useful for deriving built-up density and urban form metrics in data-scarce regions. The building points were converted into raster data and kernel density was calculated as a proxy for anthropogenic modification of the land surface.

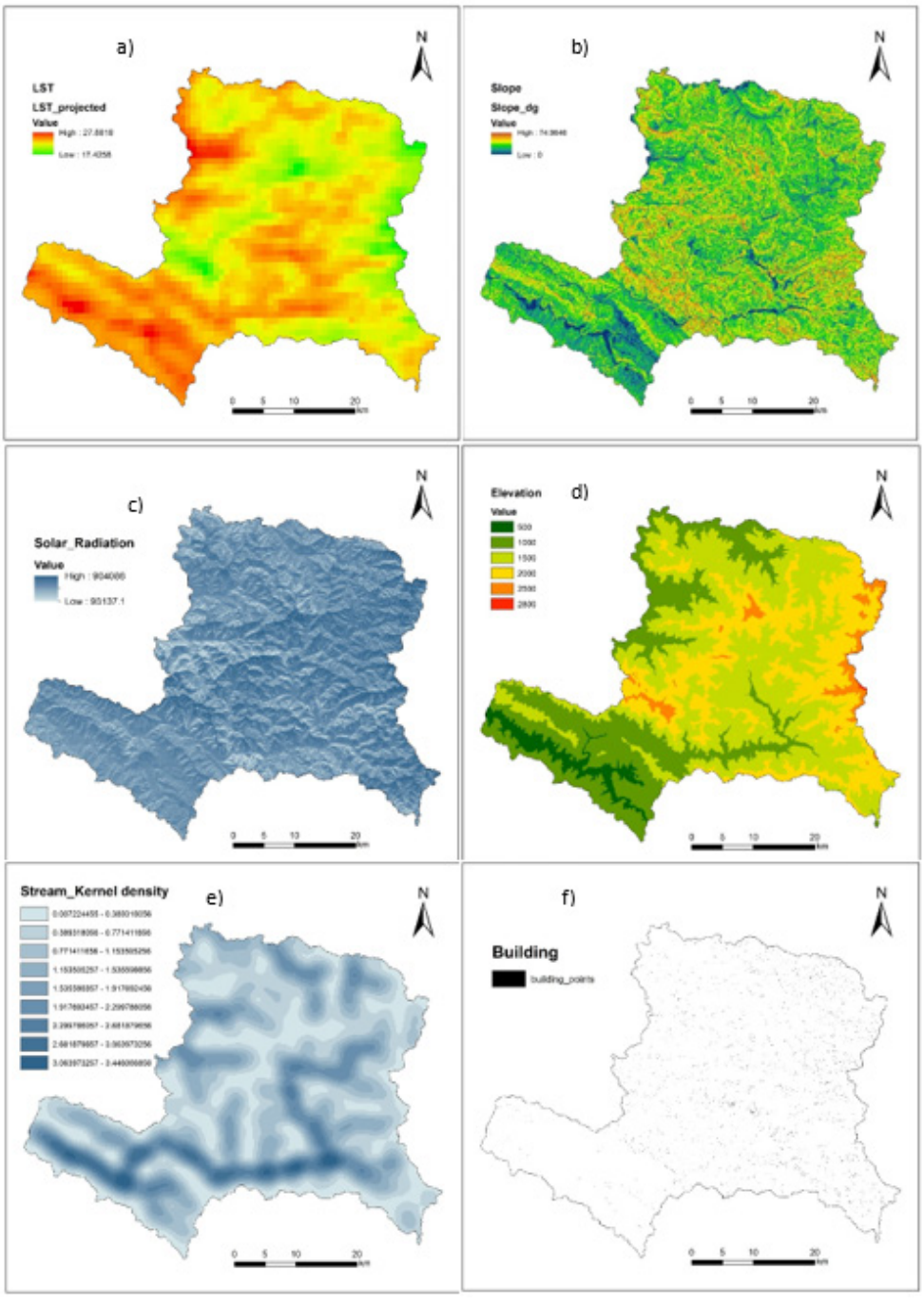

Figure 3. Independent variables: a) LST b) Slope c) solar radiation d) elevation e) Stream_kernel f) Building points

Data analysis

Global regression and GWR specification

The modeling strategy follows standard practice in spatial regression analyses of LST and then testing for spatial non-stationarity before applying GWR. LST is specified as the dependent variable, while solar radiation, elevation, slope, building density and distance to streams served as explanatory variables representing radiative forcing, topographic control, terrain steepness, built-up intensity and moisture availability, respectively. Non-stationarity and heteroscedasticity are evaluated using diagnostic tests such as the Koenker (Breusch–Pagan) statistic and spatial residual patterns in order to justify the use of GWR.

Spatial autocorrelation

A spatial dependency of the variables causes spillover effects in nearby locations. The temperature of the ground surface may be concentrated in locations with high economic activity, and other regions may exhibit similar trends. The most widely used spatial autocorrelation indicator, global Moran's I, was chosen to estimate the geographical connection. It is calculated using the following formula: (Huang Z., 2025)

$$I = \frac{n \cdot \sum_{i=1}^{n} \sum_{j=1}^{n} w_{ij} (x_i - \bar{x}) (x_j - \bar{x})}{\sum_{i=1}^{n} \sum_{j=1}^{n} w_{ij} \cdot \sum_{j=1}^{n} (x_i - \bar{x})^2}$$

Here,

n represents the total number of study units. The spatial weight matrix (Wij) assigns values based on geographic adjacency. In general, when i and j are adjacent, Wij is indicated as 1, otherwise it is 0. xi and xj denote the LST of regions i and j. The $\bar{x}$ represents the average value of LST across all regions. The worldwide Moran's I index (I) runs from -1 to 1. Typically, the greater the absolute value of the index, the stronger the geographical link. If the value is more than zero, there is a positive spatial correlation, while a value less than zero shows a negative spatial clustering pattern. When I = 0, there is no spatial correlation and LST produces a random geographical distribution:

$$Z_I = \frac{I - E(I)}{\sqrt{Var(I)}}$$

Here (I) and (I) represent the expectation and standard deviation of global Moran's I index (Huang Z., 2025).

Results and Discussion

GWR Model results

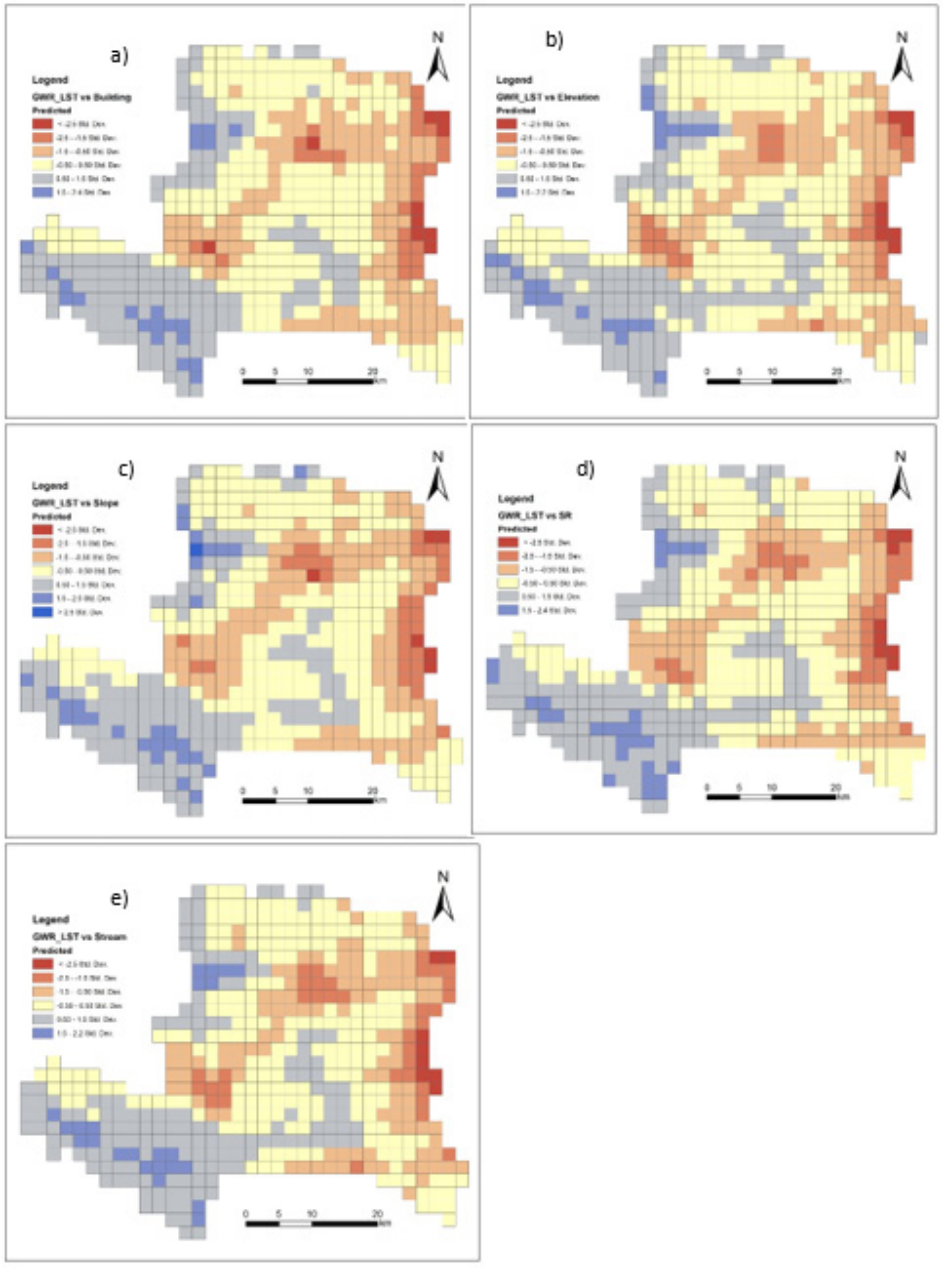

Figure 4. GWR of LST with a) Building b) Elevation c) Slope d) Solar Radiation and e) Stream

Table 2. GWR result of individual independent variable with LST.

Var name	AICc	R2	R2Adjusted	ZScore
Stream	527.262	0.934	0.889	5.486
Solar radiation	742.318	0.899	0.829	7.642
Building	672.714	0.867	0.824	10.057
Slope	689.915	0.903	0.842	5.359
Elevation	393.332	0.936	0.903	4.137

Influence of elevation

GWR modelling is done with the each five of the independent variables. Elevation exerts a strong and spatially consistent negative influence on LST across the district. This is supported by theoretical and empirical literature documenting the cooling effects associated with increasing altitude due to reduced air density, enhanced convective heat loss, and decreased atmospheric thickness (Pepin et al., 2015). In Salyan, the general topography exhibits lower values of LST, particularly in higher elevations along ridge tops. Additional cooling provided by canopy cover through evapotranspiration and shading enhances these patterns in forested highlands. The local coefficient maps provided by GWR indicate that elevation does not exert a uniform influence across the district but instead varies smoothly with the strongest negative relationships in regions with steep terrain or significant altitudinal gradients.

Influence of slope

The slope plays a complex role in shaping LST is complex and influenced by the terrain aspect and surface orientation. LST values are more common on steeper slopes due to improved drainage, higher wind exposure, and reduced heat absorption. In Salyan, GWR data show that slope exerts a moderate but spatially varied influence on LST. The cooling effect of slope is particularly prominent in areas with south-facing aspects, where steep slopes get more solar radiation yet dissipate heat more effectively. In contrast, gentle slopes or flat valley bottoms have higher LST values due to heat accumulation and limited airflow. These findings are similar with terrain-based thermal studies in other mountainous areas, which show that slope and aspect have a significant impact on surface heating patterns (Sharma et al., 2020).

Influence of solar radiation

Solar radiation is one of the strongest predictors of LST. This relationship is well documented, as radiation directly heats the ground surface. In Salyan, areas with high values of solar radiation that are common for south-facing slopes and exposed hillsides, exhibit the high values of LST. The spatial distribution of solar radiation is strongly reflected in the standardized residuals, especially in the warm residual clusters, where solar exposure seems to surpass the average

conditions represented by the model. GWR coefficient maps show that the impact of this driver is very strong for central and northern districts where the terrain opens up and allows higher fluxes of radiation.

Influence of proximity to streams

Distance to streams has a negative association with LST, that reflects the cooling of riparian ecosystems. Streams helps with evaporative cooling, greater humidity, and lower ground temperatures. In Salyan, areas close to streams consistently show lower LST values, although the strength of this effect varies. The cooling effect is stronger in larger river basins where streams are surrounded by vegetation and moist soils. Conversely, in steep gullies with limited streamside vegetation, the effect is weaker. This geographical variability emphasizes the importance to account both hydrological and vegetative factors when interpreting stream-induced thermal patterns.

Influence of building density

Building density is the concentration of the buildings on a given land area. It is the primary anthropogenic factor used in this model. The model result shows a positive association of building density with LST. The region with higher number of buildings experience increased temperatures due to shift of natural surfaces with impervious materials, the reduction of vegetation, and the emission of anthropogenic heat. In Salyan, although the settlements are relatively dispersed compared to the urban areas, the pockets of high building density occur in town centers and along the road corridors. These areas shows noticeably higher LST values, consistent with the urban heat island effect documented in global literature (Li et al., 2011). Thus, the effect of building density is more pronounced in flatter areas where structures cluster more tightly and thermal dissipation is reduced.

Overall model result

The results show that the GWR serves as an effective technique in modeling the spatial variability of LST in Salyan District. The model has a high explanatory power, with an R^2 value of 0.939 and an adjusted R^2 of 0.915, thus showing that the selected variables collectively explain a large part of spatial variation in LST. The AICc value of 308.485238 also confirms the efficiency of the model, while the residual sum of squares indicates minimal unexplained variance (Table 3). The standardized residuals visually indicate a district-wide pattern of cold and hot spots in an alternate manner to reflect the influence of terrain, land use, and settlement density (Figure 5)**.**

Similar high predictive performance and spatially varying relationships in LST modeling have been documented in previous GWR applications, where topography, land cover, and radiation have been shown to exert spatially heterogeneous effects (Fotheringham et al., 2002; Weng et al., 2007).

Table 3. GWR table

S.N	VARNAME	VARIABLE
1	ResidualSquares	32.814383
2	AICc	308.485238
3	R2	0.939007
4	R2Adjusted	0.915122
5	ZScore	2.981596
6	Moran's Index	0.092052
7	PValue	0.002867

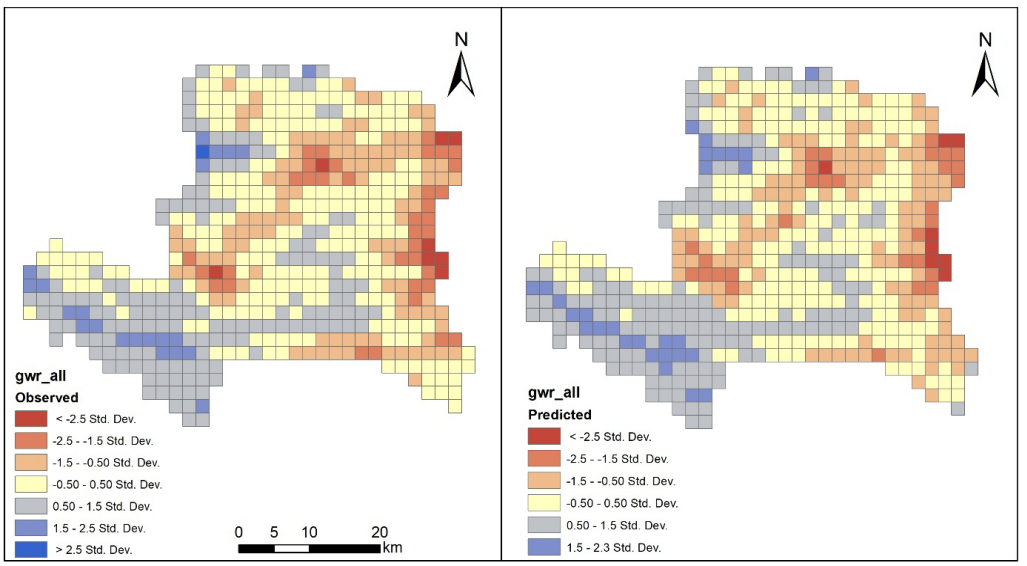

Figure 5. Observed and Predicted LST

The GWR results show significant geographical heterogeneity in the elements that influence land-surface temperature (LST), with a tight match between actual and predicted maps showing that the model efficiently captures localized thermal fluctuations (Figure 5). Higher-than-expected LST clusters in the central and eastern areas (orange-red) indicate a combination of lower elevation, increased solar radiation, and higher building density, all of which are known to exacerbate surface heating (El Garouani et al., 2021; Weng, 2009). Cooler-than-expected zones (blue), particularly in the northwest and southern regions, tend to be related with higher altitudes, steeper slopes, and closeness to streams conditions that enhance evaporative cooling and limit heat storage (Guo et al., 2020).

The spatial agreement between observed and predicted patterns (Figure 5) demonstrates GWR's superiority in capturing localized environmental controls on LST compared to global models, which is consistent with previous findings that LST drivers vary significantly across space (Fotheringham, Brunsdon & Charlton, 2002; Foody, 2004). Overall, the model identifies distinct geographic clusters where topography, hydrology, and built-environment elements influence LST on a fine spatial scale.

Model evaluation

Furthermore, the spatial autocorrelation results for land surface temperature (LST) show a Moran's I Index of 0.092, a Z-score of 2.98, and a p-value of 0.0029, indicating a statistically significant but low-to-moderate positive spatial autocorrelation.

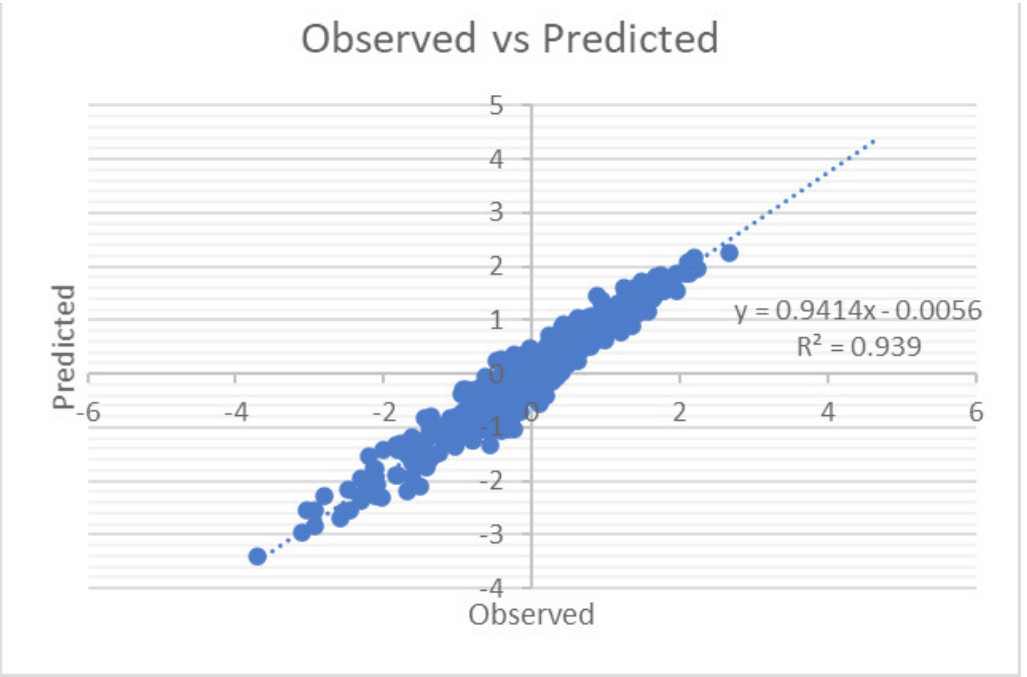

Figure 6. Observed vs Predicted values of LST by GWR

This means that LST values are not randomly distributed; instead, nearby locations tend to have slightly similar temperatures, forming mild spatial clustering. Although the Moran's I value is relatively small, the high Z-score and very low p-value confirm that the observed spatial pattern is unlikely to be due to chance, suggesting meaningful spatial processes such as terrain, land cover, and microclimatic conditions influencing LST distribution**.** Similar results have been reported in other spatial temperature studies, where urban form,

elevation, and land cover create clusters of warm or cool zones, producing modest but statistically significant positive Moran's I values (e.g., Weng et al., 2004; Zhou et al., 2019; Gupta et al., 2021).

Similarly, the observed–predicted scatter plot (Figure 6) further confirms this strong fit, as points closely align with the 1:1 line and the regression slope (0.94) indicates almost unbiased predictions.

Conclusion

The GWR analysis shows that land surface temperature patterns in Salyan District are strongly and spatially heterogeneously controlled by a combination of solar radiation, elevation, slope, building density, and distance to streams, with the model accounting for more than 90% of the observed variance in LST and showing only weak residual spatial autocorrelation. These findings highlight that both topographic setting and localized anthropogenic modification of the land surface jointly shape the district's thermal environment, implying that climate-sensitive planning should prioritize conservation of cooler high-elevation and riparian zones while managing building expansion and land-use change in thermally vulnerable areas.

References

Camilius H. F., Deus D, and Ngereja Z., (2022) Geographically weighted regression modeling of a daytime urban heat island in Dar es Salaam Metropolitan areas. *Zenodo*. http://doi.org/10.5281/zenodo.6557244

Colaninno, N., & Morello, E. (2022). Towards an operational model for estimating day and night instantaneous near-surface air temperature for urban heat island studies: Outline and assessment. *Urban Climate*, *46*, 101320. https://doi.org/10.1016/j.uclim.2022.101320

El Garouani, M., Amyay, M., Lahrach, A., & Jarar Oulidi, H.. (2021). Land surface temperature in response to land use/cover change based on remote sensing data and GIS techniques: Application to Saïss Plain, Morocco. *Journal of Ecological Engineering*, *22*(7), 100–112. https://doi.org/10.12911/22998993/139065

Eshetie, S. M.. (2024). Exploring urban land surface temperature using spatial modelling techniques: a case study of Addis Ababa city, Ethiopia. *Scientific Reports*, *14*(1). https://doi.org/10.1038/s41598-024-55121-6

Fan, Q., Song, X., Shi, Y., & Gao, R.. (2021). Influencing factors of spatial heterogeneity of land surface temperature in Nanjing, China. *IEEE Journal of Selected Topics in Applied Earth Observations and Remote Sensing*, *14*, 8341–8349. https://doi.org/10.1109/jstars.2021.3105582

Fotheringham, A. S., Brunsdon, C., & Charlton, M. (2002). *Geographically weighted regression: The analysis of spatially varying relationships*. *John Wiley & Sons. 13*.

Guo, A., Yang, J., Xiao, X., Xia (Cecilia), J., Jin, C., & Li, X. (2020). Influences of urban spatial form on urban heat island effects at the community level in China. *Sustainable Cities and Society*, *53*, 101972. https://doi.org/10.1016/j.scs.2019.101972

Gupta, S., Dey, S., & Kaushal, R. (2021). Spatial patterns and determinants of land surface temperature in a Himalayan city: A geospatial analysis. *Urban Climate, 35*, 100754.

Huang, Z., Duan, L., Xu, Y., Yang S., Lin Z., Yue H., and Yang J., (2025). Exploring the influence of urban green space and urban morphology on urban heat Islands using street view and satellite imagery. *Scientific Reports 15*, 23759 (2025). https://doi.org/10.1038/s41598-025-07904-8

Hou, L., Yue, W., & Liu, X.. (2021). Spatiotemporal patterns and drivers of summer heat island in Beijing-Tianjin-Hebei Urban Agglomeration, China. *IEEE Journal of Selected Topics in Applied Earth Observations and Remote Sensing*, 1–1. https://doi.org/10.1109/jstars.2021.3094559

Kopczewska, K. (2025). Analysing local spatial density of human activity with quick density clustering (QDC) algorithm. *Computers, Environment and Urban Systems*, *119*, 102289. https://doi.org/10.1016/j.compenvurbsys.2025.102289

Li, X., Li, Y., Di, S., Niu, Y., & Zhang, C. (2022). Evapotranspiration and land surface temperature of typical urban green spaces in a semi-humid region: Implications for green management. *Frontiers in Environmental Science*, *10*, 977084. https://doi.org/10.3389/fenvs.2022.977084

Liang, S., Cheng, J., Jia, K., Jiang, B., Liu, Q., Xiao, Z., Yao, Y., Yuan, W., Zhang, X., Zhao, X., & Zhou, J. (2021). The global land surface satellite (GLASS) product suite. *Bulletin of the American Meteorological Society*, *102*(2), E323-E337. https://doi.org/10.1175/BAMS-D-18-0341.1

Lessani, M. N., & Li, Z. (2024). SGWR: similarity and geographically weighted regression. *International Journal of Geographical Information Science*, *38*(7), 1232–1255. https://doi.org/10.1080/13658816.2024.2342319

Rao, Y., Dai, J., Dai, D., & He, Q. (2021). Effect of urban growth pattern on land surface temperature in China: A multi-scale landscape analysis of 338 cities. *Land Use Policy*, *103*, 105314. https://doi.org/10.1016/j.landusepol.2021.105314

Roba, Z. R., & Tabor, K. W. (2025). Geospatial analysis of vegetation and land surface temperature for urban heat island mitigation in Hawassa City, Ethiopia. *Scientific Reports*, *15*, 31786. https://doi.org/10.1038/s41598-025-17014-0

Duan, S., & Li, Z. (2016). Spatial downscaling of MODIS land surface temperatures using geographically weighted regression: case study in Northern China. *IEEE Transactions on Geoscience and Remote Sensing*, *54*(11), 6458–6469. https://doi.org/10.1109/tgrs.2016.2585198

Wang, H., Huang, Z., Yin, G., Bao, Y., Zhou, X., & Gao, Y. (2022). GWRBoost:A geographically weighted gradient boosting method for explainable quantification of spatially-varying relationships. *ArXiv*. https://arxiv.org/abs/2212.05814

Wang, S., Luo, X., & Peng, Y.. (2020). Spatial downscaling of MODIS land surface temperature based on geographically weighted autoregressive model. *IEEE Journal of Selected Topics in Applied Earth Observations and Remote Sensing*, *13*, 2532–2546. https://doi.org/10.1109/jstars.2020.2968809

Weng, Q. (2009). Thermal infrared remote sensing for urban climate and environmental studies: Methods, applications, and trends. *ISPRS Journal of Photogrammetry and Remote Sensing*, *64*(4), 335-344. https://doi.org/10.1016/j.isprsjprs.2009.03.007

Weng, Q., Lu, D. and Schubring, J. (2004) Estimation of land surface temperature vegetation abundance relationship for urban heat island studies. *Remote Sensing of Environment, 89,* 467-483. https://doi.org/10.1016/j.rse.2003.11.005

Xinming Z., Xiaoning S., Pei L., and Ronghai H., (2021). Spatial downscaling of land surface temperature with the multi-scale geographically weighted regression. *Journal of Remote Sensing 25(8)*: 1749-1766 doi: https://doi.org/10.11834/jrs.20211202

Yao, L., Sun, S., Song, C., Li, J., Xu, W., & Xu, Y. (2021). Understanding the spatiotemporal pattern of the urban heat island footprint in the context of urbanization, a case study in Beijing, China. *Applied Geography*, *133*, 102496. https://doi.org/10.1016/j.apgeog.2021.102496

Zhi, Y., Shan, L., Ke, L., & Yang, R.. (2020). Analysis of land surface temperature driving factors and spatial heterogeneity research based on geographically weighted regression model. *Complexity*, *2020*, 1–9. https://doi.org/10.1155/2020/2862917

Zhou, W., Qian, Y., Li, X., Li, W., & Han, L. (2013). Relationships between land cover and the surface urban heat island: seasonal variability and effects of spatial and thematic resolution of land cover data on predicting land surface temperatures. *Landscape Ecology*, *29*(1), 153–167. https://doi.org/10.1007/s10980-013-9950-5